MATERIAL AND GEOMETRIC DISPERSION EFFECTS ON LONGITUDINAL ACOUSTIC DISTURBANCES IN A DUMILOAD FOR SONAR TRANSDUCERS

Fernando L. de Magalhães
Sonar Group - Brazilian Navy Research Institute (IPqM)
mafer@gbl.com.br
Moysés Zindeluk
PEM/COPPE – Federal University of Rio de Janeiro
moyses@ufrj.br

Abstract. *Underwater acoustic transducers are usually tested in large water tanks or in deep-sea environments, where high hydrostatic pressure and free field conditions are satisfied. For hydroacoustic projectors such difficulties may be avoided by employing in laboratory devices named DUMILOAD (Dummy Mechanical Impedance Load). Presently the authors are developing an impedance load that uses a PMMA rod coupled to a Tonpilz Transducer. The system is designed to apply to the transducer an acoustic impedance similar to the radiation impedance in the water, if harmonic elastic waves are propagating in the rod. In this work the complexities related to longitudinal propagation in viscoelastic rods are analyzed, when material dispersive effects are superposed to geometric effects due to the radial inertia of the medium. To characterize the combined phenomena, theoretical results emphasize the influence of the rod radius on the phase velocity and on the attenuation factor curves defined by 1-D rheological models. The paper proposes a transfer matrix method which compensates for the phase and amplitude distortions in the DUMILOAD and is able to identify the force and the velocity responses on the transducer from strain measurements along the rod. Preliminary results demonstrate the good applicability of the DUMILOAD and the accuracy of the mechanical impedance method.*

Keywords*: longitudinal propagation, material dispersion, geometric dispersion, sonar transducer, Dumiload*

1. Introduction

Calibration processes and endurance tests of underwater acoustic transducers are usually carried out in large water tanks or in deep-sea environments, where free field and high hydrostatic pressure conditions are both satisfied. In this sense, when sonar projectors have to be tested on power limits that, due to the cavitation phenomenon, become unfeasible the use of common measuring facilities, the complexity and the high costs related to a non-trivial acoustic chamber may be avoided by employing in laboratory devices named DUMILOADs (contraction to Dummy Mechanical Impedance Loads). Two types of DUMILOAD are mentioned in the literature: "Termination Transducer Device" and "Vase with Termination Transducer" (Afonso and Magalhães, 1999). However, despite their relative simplicity and good accuracy for a narrow bandwidth over the transducer fundamental resonance, these DUMILOADs are dynamically unstable for endurance tests and restricted to low frequency applications. So, with the aim to minimize such restrictions, the authors are developing a novel type of dummy load, named Propagation Rod DUMILOAD, which uses a cylindrical rod made of polymethyl methacrylate (PMMA) as a radiation impedance medium. The device, depicted in Fig. 1, is designed to submit to a Tonpilz transducer, in the air, an acoustic load similar to the hydroacoustic impedance, when longitudinal harmonic elastic waves are propagating in the rod. The transmission versus frequency curve of the testing transducer can be defined by comparing its response with the data obtained from a reference projector measured in the rod and in the water. By adopting pulse excitation techniques, it is possible to measure the electrical immitance curves on the transducer terminals and apply endurance tests under simulated ocean conditions.

It is important to observe that, although the force and the velocity fields can be determined by strain-gages located on the cylindrical surface of a bar or rod, there are some uncertainties related to the longitudinal propagation in viscoelastic materials. Besides the attenuation of the signal due to the internal friction in the polymer structure, the propagation of non-monotonic disturbances in a bar leads to a dispersive behavior where the phase velocity increases with the frequency. The same rule is applicable to the attenuation factor. Notice that by bar it is meant that the lateral inertia of the medium can be ignored, so the propagation and its effects are only in the longitudinal direction. By rod it is meant that displacements, strains, stresses, forces and velocities are taken in the longitudinal and radial directions.

When the wavelength is of the same order or smaller than the rod diameter, the lateral inertia cannot be disregarded and the effects of another kind of dispersion, strictly geometrical, becomes significant for longitudinal propagation. For the case of a purely elastic material, the phase velocity decreases with increasing frequency, converging asymptotically to specific levels. The superposition of the material and geometric dispersion effects yields a phase velocity increasing or decreasing with frequency, according to their relative importance. As another consequence of geometric dispersion, it is well known that a longitudinal wave excited in an initially uniform condition may experiment a non-plane transversal distribution while the disturbance moves along the rod (Tyas and Watson, 2001). Such kind of distortion equally occurs

for viscoelastic rods and can be responsible for important uncertainties in the signal monitored by strain-gages, once the dynamic conditions on the rod surface do not necessarily represent the conditions at the inside particles.

Since the DUMILOAD is not a perfectly slender bar, the present work synthesizes relevant particularities concerning the longitudinal propagation in cylindrical rods when the two types of dispersion are present. To characterize the combined phenomena, the Pochhammer generalized equation (Zhao, 1992; Benatar *et al*., 2003) is solved and the influence of the rod radius on the phase velocity and on the attenuation factor is emphasized. Based on theoretical longitudinal and radial displacement fields in a PMMA rod, uncertainties related to the signal monitored in the DUMILOAD are here analyzed. In order to design the loading rod and to predict its dynamic response, this paper summarizes a mechanical impedance method where the dispersion effects are introduced by using the propagation coefficients in the displacement, strain, force and velocity expressions. In view of the fact that the method leads to a "T" distributed parameters circuit to represent a rod segment, a circuital model of the DUMILOAD is obtained, that associates the electrical excitation on the input terminals of the transducer to the power transmitted along the rod. From such an approach, some important experimental parameters and requirements for the device could be predefined, such as: amplitude of the electrical signal to be applied to the transducer, obtainable bandwidth, minimum sensitivity for the strain gages and location of the monitoring points. On the basis of analytical results, the impedance and the transmission behaviors of a DUMILOAD rods, designed for testing a 51 kHz Tonpilz transducer, are evaluated. The results are compared with the electroacoustic response of the transducer in a freshwater tank.

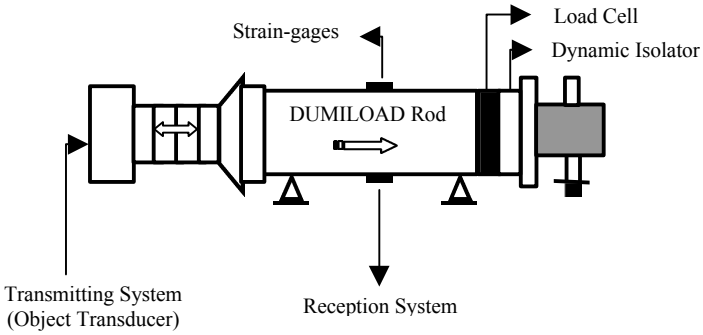

Figure 1. Propagation Rod DUMILOAD.

2. Material and geometric dispersion in a cylindrical rod

2.1. Dispersion curves

Bancroft (1941) was the first to determine the lowest longitudinal mode of the Pochhammer equation and the relation between the phase velocity and the wavenumber in an elastic cylindrical rod. Ever since, several models have been proposed to generalize the Pochhammer exact theory to a wider frequency spectrum and higher modes, or to satisfy the stresses and strains boundary conditions at the ends of finite rods. Recently, Ahmad (2004) has obtained good results with a simplified approach, developed from the exact theory, but limited to a frequency band where the phase velocity is higher than the shear wave velocity and lower than the dilatation wave velocity.

In order to apply the Pochhammer solution to the DUMILOAD device, it should be pointed out that experimental investigations have proved the good accuracy of the results when the rod length is at least 2.5 times the diameter (Coates, 1991). Moreover, although the original solution was developed for purely elastic media, Coquin (1964), Zhao (1992), and more recently Benatar *et al*. (2003), demonstrate that the Pochhammer frequency equation can be extended for linear viscoelastic rods if the elastic parameters are replaced by their complex counterpart, where the storage and the loss properties of the material are directly introduced. However, it is important to notice that the harmonic wave solution developed by Coquin is not a general one, since it is only applicable to materials for which the rheological behavior can be described by the Kelvin-Voigt model. Otherwise, Zhao solution may be generalized for cylindrical rods of any linear viscoelastic material, but it is necessary to know beforehand the complex moduli of the material over the whole frequency range of interest. A difficulty factor added to the Zhao solution is to find the complex roots involved in a two-dimensional optimization problem.

To overcome these limitations with negligible errors, Benatar *et al*. (2003) proposed a simplified Pochhammer frequency equation for low and intermediate loss viscoelastic rods (loss tangent ≤ 0.25). For this case, the Pochhammer equation with complex constitutive parameters is decoupled in two parts or two new equations: a real one, with solution leading to the phase velocity curves and an imaginary equation where the roots are related to the effects of geometric dispersion on the attenuation factor, respectively:

$$2\bar{p}\left(\bar{q}^2+\bar{k}^2\right)J_1(\bar{p})J_1(\bar{q})-\left(\bar{q}^2-\bar{k}^2\right)^2 J_0(\bar{q})-4\bar{k}^2\bar{p}\bar{q}J_1(\bar{p})J_0(\bar{q})=0 \qquad (1)$$

and

$$\begin{aligned}&2d_q\bar{k}^2\bar{p}J_1(\bar{q})J_1(\bar{p})-2d_q\bar{p}J_1(\bar{p})\left(\bar{q}^3J_0(\bar{q})+\bar{q}^2J_1(\bar{q})\right)-2d_p\bar{p}^2J_0(\bar{p})J_1(\bar{q})\left(\bar{q}^2+\bar{k}^2\right)-4d_k\bar{p}\bar{k}^2J_1(\bar{p})J_1(\bar{q})+\\&+d_qJ_0(\bar{p})\left(3\bar{q}^4J_1(\bar{q})-2\bar{q}^3\bar{k}^2J_0(\bar{q})-2\bar{q}^2\bar{k}^2J_1(\bar{q})+\bar{q}\bar{k}^4J_0(\bar{q})\right)-d_qJ_0(\bar{p})\left(\bar{k}'^4J_1(\bar{q})-\bar{q}^5J_0(\bar{q})\right)+\\&+d_p\bar{p}J_1(\bar{q})J_1(\bar{p})\left(\bar{q}^4+\bar{k}^4-2\bar{q}^2\bar{k}^2\right)-4d_k\bar{k}^2J_1(\bar{q})J_0(\bar{p})\left(\bar{q}^2-\bar{k}^2\right)-4d_q\bar{p}\bar{q}\bar{k}^2J_1(\bar{p})\left(\bar{q}J_1(\bar{q})+\tfrac{1}{2}(J_0(\bar{q}))\right)+\\&+4d_p\bar{q}\bar{p}^2\bar{k}^2J_0(\bar{p})J_0(\bar{q})+8d_k\bar{p}\bar{q}\bar{k}^2J_1(\bar{p})J_0(\bar{q})=0\end{aligned} \tag{2}$$

for

$$p^2=s_1^2b_0^2-b^2,\ \bar{p}=pa,\ q^2=s_2^2b_0^2-b^2,\ \bar{q}=qa,\ k=b-ia,\ \bar{k}=ka \tag{3}$$

$$d_p=\frac{s_1^2b_0^2d_0-b^2d_k}{s_1^2b_0^2-b^2},\ d_q=\frac{s_2^2b_0^2d_0-b^2d_k}{s_2^2b_0^2-b^2},\ b=\frac{w}{c},\ b_0=w\sqrt{\frac{r}{E}},\ s_1=\sqrt{\frac{(1+n)(1-2n)}{(1-n)}} \tag{4}$$

$$s_2=\sqrt{2(1+n)},\ d_0=\frac{E'}{2E},\ d_k=\frac{a}{b} \tag{5}$$

where a is the rod radius, b_0 is the wavenumber of a perfectly slender viscoelastic bar, b represents the real part of the complex wavenumber k, a is the attenuation factor, w is the angular frequency, c is the phase velocity, E and E' are respectively the storage and the loss functional components of the Young modulus, r is the density and n is the Poisson ratio (assumed real). d_p, d_q are the loss factors concerning the components of dilatational and shear waves in the longitudinal direction. d_0 is the loss factor of a slender viscoelastic bar of the same material and d_k is the loss factor to be determined. Notice that Eq. (1) is identical to the Pochhammer equation developed for elastic rods. In the present work, Eqs. (1) and (2) were solved numerically by using the bisection method, together with an automatic sweeping technique. To superpose the geometric dispersion to the material dispersion effects the following expressions are valid:

$$c_{mg}=\left(\frac{c_g}{c_0}\right)c_m \qquad a_{mg}=\left(\frac{a_g}{a_0}\right)a_m \tag{6}$$

The above subscripts, *m*, *g* and *mg,* indicate material dispersion, geometric dispersion and the coupling of material and geometric dispersions. c_0 and a_0 represent, respectively, the longitudinal propagation velocity, or bar velocity ($c_0=\sqrt{E/r}$), and the attenuation factor of a viscoelastic slender bar. In this work, Eq. (1) and Eq. (2) were normalized to be solved with the roots (c_g/c_0) and (a_g/a_0) as functions of frequency.

Although experimental methods have been successfully applied to characterize viscoelastic rods where material and geometric dispersive effects are superposed, in view of the good results obtained from the generalized Pochhammer equation and the high accuracy of some mechanical rheological models, a combined analytical-experimental approach is here adopted. In a development stage, it is worthwhile using this type of approach, once paramount characteristics of the propagation phenomenon in the calibration rod may be previously known. Specifically for PMMA bars, the rheological models developed by Zener (Sogabe and Tsuzuki, 1986) and Zhao (1992) lead to propagation constant curves of significantly good agreement with experimental data published in other references, see for instance Hillström *et al*. (2000). Concerning the topological difference between the models, while Zhao uses four Kelvin-Voigt cells in series with one spring element, the classical Zener model adopts only one Kelvin-Voigt cell and one spring in series. Notice that the solution of the Zener model was based on parameters defined in four different papers and tabled in Sogabe and Tsuzuki (1986). In Fig. 2, the wavenumber and the attenuation factor of a perfectly slender PMMA bar are depicted, according to the two models. In terms of bar wavenumber (b_0), by comparing the analytical curves shown in Fig. 2 with data published in Hillström *et al.* (2000), it is proved that all of the spring-dashpot coefficients used in the models give satisfactory results. Considering the attenuation factor a_0, it should be underlined that the results calculated from the Zhao model are in particularly good agreement with the experimental ones.

Figure 3.a shows the solution of Eq. (1) for the first three longitudinal modes in a PMMA rod, symbolized by $M_{1,n}$ where *n* indicates the mode order. Evidently, the smaller is the radius, the higher are the cut-off frequencies for the second and third modes. To obtain the coupled phase velocity curve from Eq. (6.a), the roots of the Pochhammer equation corresponding to the first longitudinal propagation mode (Young mode) are combined with the phase velocity curve defined through the Zhao model, resulting in Fig. 3.b. According to experimental results (Redwood, 1960), when one of the rod ends is excited by longitudinal loads with a uniform distribution along the cross-section, all of the modes

are evanescent, excepting the Young mode. Each of such modes may experiment a propagating behavior only when the excitation load is applied over very small annular portions of the cross-section of the rod and above its corresponding cut-off frequency. If a Tonpilz transducer is used as the excitation source, the amplitudes related to the flapping of the front mass up to frequencies around the first transduction mode are probably of minor importance when compared to the longitudinal displacement of the dynamic parts as a whole (Magalhães and Afonso, 2001). So, in terms of propagation conditions in the DUMILOAD rod, the analytical model can be restricted to the Young mode. Figure 3.b proves that the smaller the radius, the more the coupled dispersion curve tends to the material dispersion curve and, in consequence, the wider is the bandwidth where the phase velocity is higher than the bar velocity. On the other hand, the curves demonstrate that a PMMA rod is strongly affected by geometric dispersion effects, loosing the almost monotonic growing of phase velocity even for the first frequency decades. Taking the 50 mm radius curve as reference, one may observe that for frequency components around 10 kHz even a narrow band disturbance may be distorted while propagating along the rod. The superposed dispersion curve converges to a propagation velocity a little higher than Rayleigh surface waves (≈ 0.56 m/s) in elastic rods.

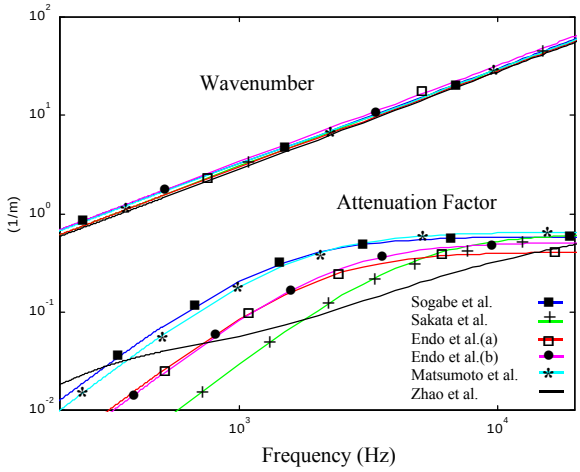

Figure 2. Wavenumber and attenuation factor of a PMMA bar by solution of the Zener model and the Zhao model.

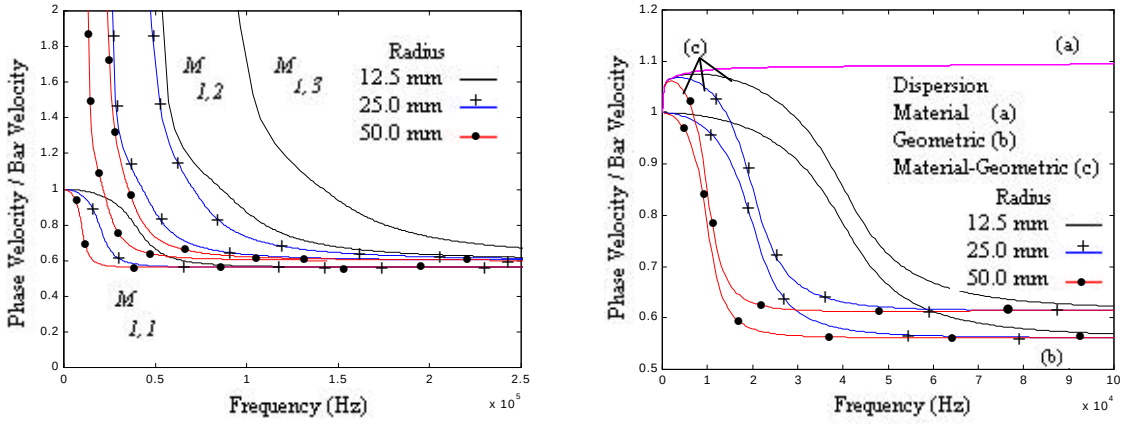

Figure 3. Normalized phase velocity curves for (a) pure geometric dispersion in rods of Poisson's ratio 0.4 and for (b) material dispersion in a PMMA bar and material-geometric dispersion in PMMA rods.

Figure 4.a shows the attenuation amplification factor a_g / a_0 determined in Eq. (2). It is interesting to notice that, despite being the amplitude of the peak points independent of the rod radius, they are wider and centered at higher frequencies for smaller cross-sections. The superposition of these curves with that one concerning the Zhao model, in Fig. 2, results in the attenuation factor curves for a PMMA rod, indicated in Fig. 4.b. As the curves point out, depending on the frequency the geometric effect in amplifying the attenuation factor is not necessarily a growing function of the radius. The data implemented in Fig. 2, Fig. 3 and Fig. 4 are used in the DUMILOAD design and for simulating the transmission response of the rod.

2.2. Longitudinal and radial displacement fields

In this work, to preview the (axysimmetric) displacement distribution throughout a cross-section of a linear viscoelastic rod, the equations developed for elastic media (Tyas and Watson, 2001) receive a mathematical treatment

similar to that one adopted in the generalized Pochhammer theory. Excepting the Poisson ratio, an imaginary term added to all of the constitutive parameters denotes the material internal damping. In terms of longitudinal displacement, the amplitude is given by:

$$U = g\ A \frac{J_1(\tilde{p}a)}{\tilde{p}a} \frac{\tilde{p}a J_0(\tilde{p}r)}{J_1(\tilde{p}a)} + \frac{(1-SZ)}{(Z-1)} \frac{\tilde{q}a J_0(\tilde{q}r)}{J_1(\tilde{q}a)} \tag{7}$$

$$g = ik = iw/\tilde{c} = iw\sqrt{r/\tilde{E}}\ ,\ \tilde{E} = E + iE'\ ,\ \tilde{p}^2 = \frac{r\, s_1^2 w^2}{\tilde{E}} - k^2\ ,\ \tilde{q}^2 = \frac{r\, s_2^2 w^2}{\tilde{E}} - k^2 \tag{8}$$

$$S = \frac{(1-2n)}{(1-n)}\ ,\ Z = (1+n)\left(\frac{c}{c_0}\right)^2 \tag{9}$$

where r is the radial position along a cross-section. Concerning the amplitude of the radial component in a viscoelastic rod, one obtain:

$$W = ig\ A \frac{J_1(\tilde{p}a)}{\tilde{p}a} (SZ-1)^{0.5} \frac{\tilde{p}aJ_1(\tilde{p}r)}{J_1(\tilde{p}a)} - \frac{(1-SZ)}{(Z-1)} \frac{1}{(2Z-1)^{0.5}} \frac{\tilde{q}aJ_1(\tilde{q}r)}{J_1(\tilde{q}a)} \tag{10}$$

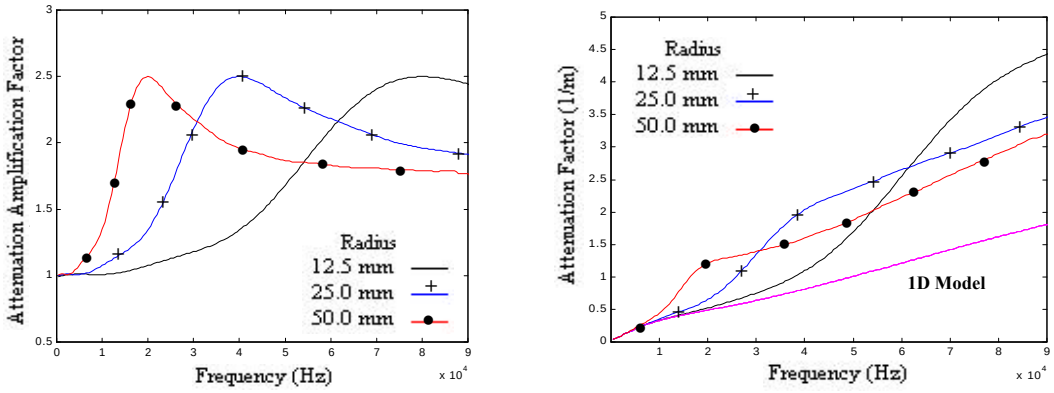

(a) (b)

Figure 4. Attenuation amplification factor curves (a) and attenuation factor curves (b) for a PMMA bar and PMMA rods. Generalized Pochhammer theory and Zhao rheological model.

Figure 5.a shows the longitudinal displacement field along the cross-section of a PMMA rod as a function of the ratio radius/wavelength (a/L). The curves correspond to the Young mode and were defined by inserting the roots of Eqs. (1) and (2) in Eq. (7). To normalize the results, the amplitude distribution is divided by the axial longitudinal amplitude. It can be noticed that, for $a/L \leq 0.1$, the displacement field is almost constant and therefore the initial plane condition of the propagating wave is practically maintained. For $a/L = 0.1$ the longitudinal amplitude on the rod surface is nearly 92.6% of the amplitude at the center point. As expected, the smaller the wavelength, the less homogeneous is the longitudinal displacement field. Another aspect related to the frequency rise is the progressive reduction of the longitudinal displacement on the rod surface ($r = \pm a$), going to zero for $a/L \approx 0.4$. Above this value the longitudinal displacements on the peripheral region and at the center are in opposite directions, so defining a nodal circumference in the rod. For the curves representing $a/L = 0.8$ and $a/L = 1.0$ the nodal circumference is located between $0.84a$ and $0.86a$. For $a/L > 1.0$ the disturbance migrates to the surface characterizing Rayleigh waves.

Figure 5.b. summarizes the correspondence between the radial displacement along a cross-section and the longitudinal displacement in the rod axis. For ratios a/L up to 0.2 the curves are quasi-linear radial functions, with a behavior that is intrinsic to plane waves. On the other hand, for a/L above 0.3 it is clear that, the smaller the wavelength, the more non-linear are the curves, and the higher are the radial displacements when compared to the longitudinal displacement at the center of the cross-sections. For $a/L = 1.0$ the radial displacement in a circumference of radius $0.81a$ is 1.7 times the longitudinal displacement in the rod axis, also characterizing a superficial propagation phenomenon. By comparing Figs. 5.a and 5.b, it can be observed the importance of using a 90° double rosette strain-gage to monitor the signal in the DUMILOAD rod. The gage elements should be aligned to the longitudinal and radial directions. For instance, considering $a/L \approx 0.4$ and the dynamic response on the rod surface, it may be proved that, while the amplitude is nearly zero in the longitudinal direction, the radial amplitude is around 0.7, both with the same

normalization factor. Notice that the difference between the longitudinal and radial amplitudes is the same in terms of strain.

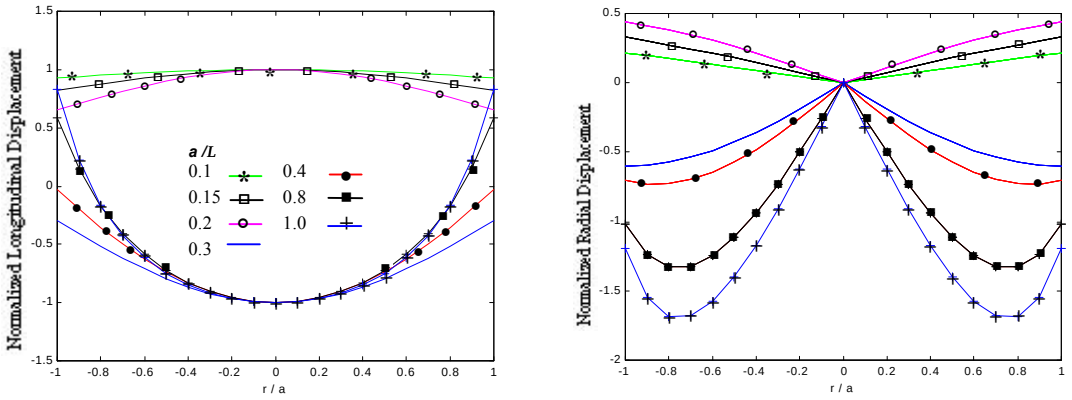

(a) (b)

Figure 5. Longitudinal (a) and radial (b) displacement fields in a PMMA rod. Generalized Pochhammer theory and Zhao rheological model.

3. Mechanical impedance method

For a uniform linearly viscoelastic rod with longitudinal harmonic propagation, the solution of the wave equation in the frequency domain leads to the following equations for the longitudinal force and the longitudinal particle velocity in a cross-section z:

$$\hat{F}_z(z,w) = \frac{rw^2}{g^2} A\left[\hat{e}_{z,p}(w)e^{-gz} + \hat{e}_{z,n}(w)e^{gz}\right] \qquad \hat{V}_z(z,w) = -\frac{iw}{g}\left[\hat{e}_{z,p}(w)e^{-gz} - \hat{e}_{z,n}(w)e^{gz}\right] \quad (11)$$

where A is the cross-sectional area of the rod and $\hat{e}_{z,p}(w), \hat{e}_{z,n}(w)$ are the Fourier transforms of the strain signals in the direction of increasing and decreasing Z coordinate, taken on the rod symmetry axis. It is important to observe that, in spite of being unidimensional equations, the material and geometric dispersion effects are partially introduced in the model by the propagation constant g. This kind of approach can be based on propagation constants defined from the generalized Pochhammer equation combined with rheological models, as proposed in the present work, or can be carried out by adopting propagation constants experimentally determined.

From the concepts of input and transfer impedances, the equations above result in a global transfer matrix where the force and velocity fields in a point or rod segment can be defined as functions of the force and velocity fields in another point or segment of the same rod. For a rod with (m-n+1) segments, the relation between the state vector at the right of segment m and the state vector on the left of segment n (m>n) is given by:

$$\begin{Bmatrix} F_z \\ V_z \end{Bmatrix}_n^e = \prod_{i=n}^{m} \begin{bmatrix} \cosh g\,l & \widetilde{Z}_0 \operatorname{senh} g\,l \\ \dfrac{\operatorname{senh} g\,l}{\widetilde{Z}_0} & \cosh g\,l \end{bmatrix}_i \begin{Bmatrix} F_z \\ V_z \end{Bmatrix}_m^d \quad (12)$$

where $\widetilde{Z}_0 = (ir\,Aw)/g$ is the characteristic impedance. Due to the acoustical reciprocity of a linearly viscoelastic rod segment, when the transfer matrix is to be applied from the left of n to the right of m, the matrix elements in the secondary diagonal assume a the negative signal. Such properties are inherent to passive, linear four-pole networks and lead to a rod segment to be represented as a "T" distributed circuit. So, a multiple segmented rod can be represented by "T" circuits associated in cascade. Equation (12) is equally applied in the time domain.

Concerning the DUMILOAD, notice that a two-diameters rod is the simplest configuration able to simulate the complex nature of the acoustic impedance in water. While the rod segment coupled to the transducer face represents the reactive term, the other segment, longer than the first, simulates the acoustic radiation. By modeling a Tonpilz transducer as a lumped electromechanical circuit around its transduction resonance, one can define the acoustic response of the whole DUMILOAD device through the global circuit shown in Fig. 6. For the case of a constant diameter rod, the circuit in Fig. 6 presents only a load impedance (Z_c) coupled to the transducer circuit.

4. DUMILOAD response in the half-power transmission band of a Tonpilz transducer

In order to exemplify the impedance capacity of the DUMILOAD rod, the global circuit shown in Fig. 6 was solved for a 51 kHz Tonpilz transducer. Notice that, besides the equivalent electromechanical circuit theory, the finite

element/boundary element methods (FEM/BEM) were also applied to predict the transducer behavior in water (Magalhães and Afonso, 2001). For the immitance and transmission responses, the results obtained from the equivalent circuit are in very high agreement with the experimental data measured for the transducer in a fresh water tank. So, eventual discrepancies in the results would be due only to the loading rod design or modeling. Moreover, from the FEM/BEM the acoustic radiation curves were obtained, in the half-power band of the transducer and it was proved that the flapping displacements of the front mass are of small amplitude when compared with the longitudinal displacement of the whole transduction set. Based on such results, the propagation constant curves presented in Section 2 and the input impedance formulation defined from Eq. (12) lead to four different loading rod designs. While the rods 1 and 2 are dimensioned considering material and geometric dispersion, for the rods 3 and 4 the effects of geometric dispersion are ignored. DUMILOADs 1 and 3 are two-diameters rods, 2 and 4 are one-diameter rods.

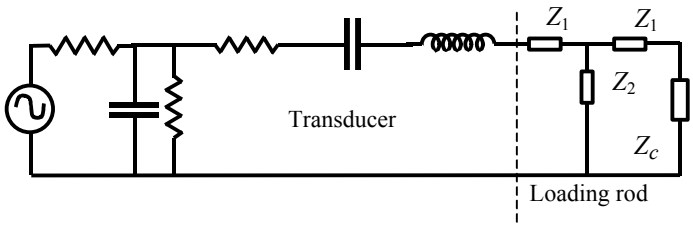

Figure 6. Electromechanical equivalent circuit for a Tonpilz transducer coupled to a two-diameter DUMILOAD.

Figure 7 compares the experimental admittance curves with the curves calculated from the equivalent circuit represented in Fig. 6. Such results demonstrate that the impedance response of the two-diameter rods is near the water impedance, despite presenting a half-power band that is 20% narrower. This discrepancy and the 10% discrepancy in amplitude between the experimental conductance curve and the curves of the rods 1 and 3 can be reduced by thickening the reactive segment and/or increasing the difference of diameter between the two rod segments. Due to the absence of mass loading, the conductance curves related to the rods 2 and 4 are of higher amplitude than the conductance in the water and both are shifted to the right when compared to the last. From the susceptance curves, it is clear that due to the reactive segments of the rods 1 and 3 the transducer may resonate around 51 kHz, as in water. Otherwise, once the radiation field is preponderantly resistive, almost all of the transducer's reactive response is related to the reactance of its front mass alone. This explains the proximity between the susceptance curves for the one-diameter and two-diameters rods.

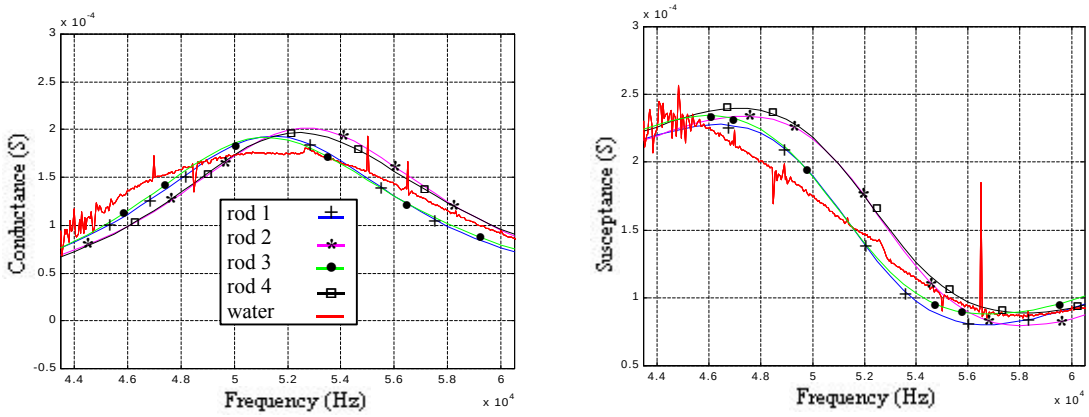

Figure 7. Conductance (a) and susceptance (b) curves on the transducer terminals.

Figure 8 shows the transmission response of the transducer when loaded by water and by the rods. To confront the analytical results with the experimental data the same directivity index was adopted for the transducer in water and facing the rods, what obviously does not represent the real propagation condition in the DUMILOAD. However, the good agreement between the curves indicates that the resistive load of the propagation rods is well adjusted to the reference values in water.

5. Conclusions

In this work a novel type of dummy mechanical load has been proposed, to simulate the hydroacoustic impedance to a Tonpilz transducer. In view of the fact that the device uses a PMMA rod as a longitudinal propagation medium, the calibration signal is invariably submitted to material dispersion effects and, depending on the radial inertia influence, also submitted to geometric dispersion. Such effects are here analyzed by combining rheological models, adjusted experimentally, with the Pochhammer generalized solution for linear viscoelastic rods. The good agreement between the analytical curves and the experimental data published in the literature makes it possible to design DUMILOAD rods

based on the propagation constants obtained. It was also shown that, depending on the ratio rod radius/wavelength, the signal extracted by strain-gages on the rod surface may not represent the conditions throughout a cross-section. In this case, the non-planar characteristics of the disturbance may be minimized by adopting double rosette strain-gages with longitudinal and radial elements and by applying correction factors for the amplitude of the Fourier components. Such factors should permit the averaging of the stress over the rod cross-section. Moreover, with the aim to model the propagation behavior, a matrix transfer method was summarized, that defines the electrical immitance curves on the transducer terminals and the transmission response along the rod. In this sense, to illustrate the method and the loading capacity of a DUMILOAD rod, four different devices were modeled. The proximity of the analytical results to the experimental ones, obtained in a fresh water tank, points out to the applicability of the Propagation Rod DUMILOAD. Otherwise, since the differences between the results for rods modeled with and without geometric dispersion are emphasized for greater distances from the transducer face, experimental investigations need to be carried to establish the effective importance of the lateral inertia on the DUMILOAD rod response.

Presently, a DUMILOAD calibration bench is being assembled. In consequence, not only the testing process metrological parameters will be assessed but experimental data will be also obtained to evaluate the theoretical models proposed.

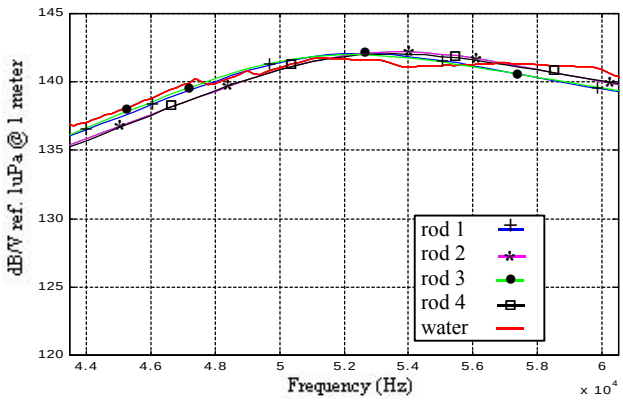

Figure 8. Transmission response curves of the transducer when loaded by water and by the rods.

6. References

Afonso, O.J.R. and Magalhães, F.L., 1999, "Development of a Mechanical Impedance Technique for High Power Performance Tests of Hydroacoustic Transducers in Air", Proceedings of the 15th Brazilian Congress of Mechanical Engineering, CD-ROM, Águas de Lindóia, Brazil.

Ahmad, F., 2004, "A Simple Formula for the Longitudinal Modes in a Cylinder", Journal of Acoustical Society of America, Vol. 115, No. 2, pp. 475-477.

Bancroft, D., 1941, "The Velocity of Longitudinal Waves in Cylindrical Bars", Physical Review, Vol. 59, pp. 588-593.

Benatar, A., Rittel, D. and Yarin, A.L., 2003, "Theoretical and Experimental Analysis of Longitudinal Wave Propagation in Cylindrical Viscoelastic Rods", Mechanics and Physics of Solids, Vol. 51, No. 8, pp. 1413-1431.

Coates, R., 1991, "The Design of Transducers and Arrays for Underwater Data Transmission", IEEE Journal of Oceanic Engineering, Vol. 16, No. 1, pp.123-135.

Coquin, G.A., 1964, "Attenuation of Guided Waves in Isotropic Viscoelastic Materials", Journal of Acoustical Society of America, Vol. 36, No. 6, pp. 1074-1080.

Hillström, L., Mossberg, M. and Lundberg, B., 2000, "Identification of Complex Modulus from Measured Strains on an Axially Impacted Bar Using Least Squares", Journal of Sound and Vibration, Vol. 230, No.3, pp. 689-707.

Magalhães, F.L. and Afonso, O. J. R., 2001, "Design of Sonar Transducers, Conventional and Non-Conventional, by Using the Finite Element/Boundary Element Methods", Proceedings of the 16th Brazilian Congress of Mechanical Engineering, CD-ROM, Uberlândia, Brazil.

Redwood, M., 1960, "Mechanical Waveguides", Ed. Pergamon Press, Bristol, UK, 300 p.

Sogabe, Y. and Tsuzuki, M., 1986, "Identification of the Dynamic Properties of Linear Viscoelastic Materials by the Wave Propagation Testing", Bulletin of JSME, Vol. 254, pp.2410-2417.

Tyas, A. and Watson, A., 2001, "An Investigation of Frequency Domain Dispersion Correction of Pressure Bar Signals", International Journal of Impact Engineering, Vol. 25, pp. 87-101.

Zhao, H., 1992, "Analyse de l'essai aux Barres d'Hopkinson – Application à la Mesure du Comportement Dynamique des Matériaux", Ph.D. dissertation, Ecole Polytechnique du Paris, Paris, France.

7. Responsibility notice

The authors are the only responsible for the printed material included in this paper.